Pharm Res (2011) 28:1905–1918
DOI 10.1007/s11095-011-0418-5

RESEARCH PAPER

Regioselective Glucuronidation of Flavonols by Six Human UGT1A Isoforms

Baojian Wu • Beibei Xu • Ming Hu

Received: 1 December 2010 / Accepted: 4 March 2011 / Published online: 7 April 2011

ABSTRACT

Purpose Glucuronidation is a major barrier to flavonoid bioavailability; understanding its regiospecificity and reaction kinetics would greatly enhance our ability to model and predict flavonoid disposition. We aimed to determine the regioselective glucuronidation of four model flavonols using six expressed human UGT1A isoforms (UGT1A1, 1A3, 1A7, 1A8, 1A9, 1A10).

Methods *In vitro* reaction kinetic profiles of six UGT1A-mediated metabolism of four flavonols (all with 7-OH group) were characterized; kinetic parameters (K_m, V_{max} and $CL_{int} = V_{max}/K_m$) were determined.

Results UGT1A1 and 1A3 regioselectively metabolized the 7-OH group, whereas UGT1A7, 1A8, 1A9 and 1A10 preferred to glucuronidate the 3-OH group. UGT1A1 and 1A9 were the most efficient conjugating enzymes with K_m values of ≤1 μM and relative catalytic efficiency ratios of ≥5.5. Glucuronidation by UGT1As displayed surprisingly strong substrate inhibition. In particular, K_{si} values (substrate inhibition constant) were less than 5.4 μM for UGT1A1-mediated metabolism.

Conclusion UGT1A isoforms displayed distinct positional preferences between 3-OH and 7-OH of flavonols. Differentiated kinetic properties between 3-*O*- and 7-*O*- glucuronidation suggested that (at least) two distinct binding modes within the catalytic domain were possible. The existence of multiple binding modes should provide better "expert" knowledge to model and predict UGT1A-mediated glucuronidation.

KEY WORDS flavonols · glucuronidation · regioselectivity · substrate inhibition · UGTs

ABBREVIATIONS

DHF	dihydroxyflavone
MS	mass spectroscopy
NMR	nuclear magnetic resonance
QHF	tetrahydroxyflavone
QSAR	quantitative structure activity relationship
S_N2	bimolecular nucleophilic substitution
THF	trihydroxyflavone
UDPGA	uridine diphosphoglucuronic acid
UGTs	UDP-glucuronosyltransferases
UPLC	ultra performance liquid chromatography

INTRODUCTION

Consumption of dietary flavonoids such as flavonols, flavones and isoflavones are associated with health benefits against ailments such as cancer and heart diseases (1,2). However, rapid glucuronidation of flavonoids in both liver and intestine leads to the presence of mainly phase II conjugates such as glucuronides and sulfates rather than the parent compound in the systemic circulation (3). As a consequence, flavonoids such as genistein and kaempferol have very poor (less than 5%) *in vivo* bioavailabilities in animals and humans (4,5), which limit their uses as therapeutic agents.

Electronic Supplementary Material The online version of this article (doi:10.1007/s11095-011-0418-5) contains supplementary material, which is available to authorized users.

B. Wu • B. Xu • M. Hu (✉)
Department of Pharmacological and Pharmaceutical Sciences
College of Pharmacy, University of Houston
1441 Moursund Street
Houston, Texas 77030, USA
e-mail: mhu@uh.edu

Glucuronidation is a major metabolic pathway, either as a primary or secondary (sequential) process in the disposition of xenobiotics (6). It is catalyzed by UDP-glucuronosyltransferases (UGTs), following a S_N2 mechanism (7). On the basis of amino acid sequence identity, human UGTs are classified into four families: UGT1, UGT2, UGT3, and UGT8 (8). The most important drug-conjugating UGTs belong to the UGT1 and UGT2 families. The human UGT1A gene cluster, located on chromosome 2q37, spans approximately 200 kb. It contains 13 individual promoters/first exons and shared exons 2–5. Each exon 1 spliced to exons 2–5 is regarded as a unique gene which translates into the corresponding active UGT1A isoform excluding the pseudogenes (i.e., UGT1A2p, UGT1A11p, UGT1A12p and UGT1A13p). Among the UGT1A family, 1A8 and 1A10 are expressed almost exclusively in the gastrointestinal tract; 1A3, 1A4 and 1A9 are primarily present in the liver; and 1A7 is mainly distributed in the stomach and esophagus. In contrast, 1A1 and 1A6 are ubiquitously present in many tissues including the liver and gastrointestinal tract (9,10).

Glucuronidation phenotyping using recombinant UGT isoforms had been widely applied in a variety of areas to (a) determine the major metabolic pathway of a particular drug (11,12); (b) identify the main isoform(s) responsible for glucuronidation of a drug (13); (c) correlate glucuronidation between organ and isoform levels (14,15); and (d) model substrate specificity of various UGT isoforms, unraveling the structural requirements for a UGT substrate (16). The QSAR regression models indicated that substrate hydrophobicity was essential for glucuronidation, which agreed with the location of UGT on the luminal side of the endoplasmic reticulum (17). The pharmacophore models identified two key hydrophobic regions adjacent from the site of glucuronidation as the substrate features for UGTs recognition (18).

The UGT1A subfamily (except UGT1A4 and 1A6) is mainly responsible for glucuronidating flavonoids, and the substrate specificity shows extensive overlaps (14,19). UGT1A4 exclusively metabolizes amine-containing compounds (20), whereas UGT1A6 exhibits limited substrate specificity for flavonoids (21). UGT1As catalyze the formation of conjugative derivatives (i.e., glucuronides) by transferring glucuronic acid from the cofactor UDP-glucuronic acid (UDPGA) to the hydroxyl oxygen(s). Multiple mono-glucuronide isomers are often generated from a single flavonoid that bears more than one conjugation site (22,23), because the aglycone-binding domain might permit multiple binding modes of the acceptor substrate (24). Some key structural features have been uncovered to govern the glucuronidation regioselectivity (or positional preference). For example, the 3′-OH group is the major determinant of the regioselectivity of flavonoid glucuronidation by UGT1A1. Flavonoids lacking a 3′-OH group were glucuronidated only at position 7-OH, while those containing this group also formed 3′-*O*-glucuronides and sometimes 4′-*O*-glucuronides (23). Consistent with this observation, human intestinal UGTs including UGT1A1 and 1A8 were especially effective in conjugating the 3′,4′ catechol unit of flavonoids (22).

Most flavonoids bear more than one potential glucuronidation site (i.e., aromatic hydroxyl groups); this presents a major challenge to the computational modeling of substrate specificity in regard to UGT metabolism. Recently, we have shown that it is necessary to model the regiospecific glucuronidation separately in order to predict the glucuronidation rates of flavonoids (25). It is also recognized that more efforts will be needed to clarify the differences between isoform-specific flavonoid metabolism including regioselectivity (so-called "expert knowledge"); this can be used to guide the development of predictive models for UGT metabolism. As a part of the continuing efforts, this paper investigated the kinetics of six UGT1A isoforms (UGT1A1, 1A3, 1A7, 1A8, 1A9 and 1A10) using selected flavonoids all having both 3-OH and 7-OH groups to evaluate regioselectivity of each UGT isoform. The six UGT1A isoforms were chosen here because of their significant contribution to glucuronidation of flavonoids shown in previous studies (14,15,19).

MATERIALS AND METHODS

Materials

Expressed human UGT isoforms (Supersomes™, i.e., UGT1A1, 1A3, 1A7-1A10) were purchased from BD Biosciences (Woburn, MA). Rabbit anti-human UGT1A polyclonal (H-300) and rabbit anti-goat IgG-HRP antibodies were purchased from Santa Cruz Biotechnology (Santa Cruz, CA). Uridine diphosphoglucuronic acid (UDPGA), alamethicin, D-saccharic-1,4-lactone monohydrate, and magnesium chloride were purchased from Sigma-Aldrich (St Louis, MO). Ammonium acetate was purchased from J. T. Baker (Phillipsburg, NT). Four (4) flavonols (Fig. 1) containing both 3-OH and 7-OH groups (i.e., 3,7-dihydroxyflavone (3,7DHF), 3,5,7-trihydroxyflavone, (3,5,7THF) 3,7,4′-tryhydroxyflavone (3,7,4′THF), and 3,5,7,4′-tetrahydroxyflavone(3,5,7,4′QHF)) were purchased from Indofine Chemicals (Somerville, NJ). All other materials (typically analytical grade or better) were used as received.

Immunoblotting

The recombinant UGT Supersomes™ (20 μg protein) were analyzed by SDS-polyacrylamide gel electrophoresis (10% acrylamide gels) and transferred onto PVDF membranes

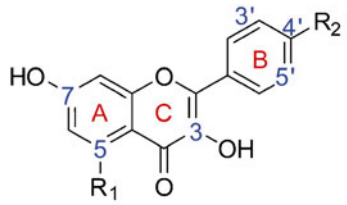

R_1	R_2	Compounds
H	H	3,7-dihydroxyflavone (3,7DHF)
OH	H	3,5,7-trihydroxyflavone (3,5,7THF or Galangin)
H	OH	3,7,4'-trihydroxyflavone (3,7,4'THF or Resokaempferol)
OH	OH	3,5,7,4'-tetrahydroxyflavone (3,5,7,4'QHF or Kaempferol)

Fig. 1 Chemical structures of the model flavonols. 3-OH of C-ring and 7-OH of A-ring are the more favorable positions for glucuronidation by UGT1As.

(Millipore, Bedford, MA). Blots were probed with anti-UGT1A antibody (H-300) that recognize all UGT1A isoforms (Santa Cruz Biotechnology, Santa Cruz, CA), followed by horseradish peroxidase-conjugated rabbit anti-goat IgG (Santa Cruz Biotechnology, Santa Cruz, CA). Membranes were analyzed on a FluorChem FC Imaging System (Alpha Innotech), and intensities of UGT bands were measured by densitometry using the AlphaEase software.

Glucuronidation Kinetics

Enzyme kinetic parameters of glucuronidation by selected UGT1A isoforms (i.e., UGT1A1, 1A3, 1A7, 1A8, 1A9, and 1A10) were determined by measuring initial glucuronidation rates of flavonols at a series of concentrations. The experimental procedures of UGT assays were exactly the same as our previous publications (14,19,26). Glucuronide formation was verified to be linear with respect to incubation time (5–60 mins) and protein concentration (13–53 μg/ml). Glucuronidation rates were calculated as nmol glucuronide(s) formed per Supersomes™ protein amount per reaction time (in unit of nmol/mg protein/min), as the actual enzyme concentration is unknown. The aglycone substrate concentrations in the range of 0.039–40 μM were used unless method sensitivity or substrate solubility necessitated otherwise. All experiments were performed in triplicates.

UPLC Analysis of Flavonols and Glucuronides

The Waters ACQUITY™ UPLC (Ultra Performance Liquid Chromatography) system was used to analyze the parent compounds and their glucuronides. UPLC methods for each flavonol and the glucuronide(s) were essentially the same as our publication (26), with slight modifications. Briefly, the mobile phase A (A) was 2.5 mM ammonium acetate in purified water (pH=6.5). Mobile phase B (B) was 100% acetonitrile. The mobile phase was run 5 min at a flow rate of 0.45 ml/min with the pre-determined gradient (0 min, 10%B; 0 to 2 min, 10–20%B; 2 to 3 min, 20–40%B; 3 to 3.5 min 40–50%B; 3.5 to 4 min, 50%–90%B; 4 to 4.5 min, 90%B; 4.5 to 5 min, 90–10%). For 3,5,7,4′QHF (kaempferol), a different mobile phase B and gradient was adopted: mobile phase B, 100% methanol; and gradient, 0 min, 10% B; 0 to 2 min, 10–20%B; 2 to 3 min, 20–40%B; 3 to 3.5 min, 40–50%B; 3.5 to 4 min, 50–70%B; 4 to 5 min, 70–90%B; 5 to 5.5 min, 90%B; and 5.5 to 6 min, 90–10%B. Quantitation of the glucuronide was based on the standard curve of the parent compound and further calibrated using the conversion factor as described earlier (19,26). The following is a list of the conversion factors used: 3,7DHF-3-*O*-glucuronide, 1.29; 3,7DHF-7-*O*-glucuronide, 0.86; 3,7,4′THF-3-*O*-glucuronide, 1.10; 3,7,4′THF-7-*O*-glucuronide, 0.92; 3,5,7THF-3-*O*-glucuronide, 0.71; 3,5,7THF-7-*O*-glucuronide, 1.41; 3,5,7,4′QHF-3-*O*-glucuronide, 1.00; 3,5,7,4′QHF-7-*O*-glucuronide, 0.70. Representative chromatograms and their UV spectra were shown in Fig. 2.

Glucuronide Structure Identification

Glucuronide structures were identified using three independent methods in a sequential process as summarized in our earlier publication (26). First, the glucuronides were confirmed by its complete hydrolysis to the aglycones when β-D-glucuronidase was used. Second, the glucuronides were identified as mono-glucuronides which showed a mass of [(aglycone's mass)+176] Da using UPLC/MS/MS. 176 Da is the mass of single glucuronic acid. Third, the sites of glucuronidation were confirmed by the "UV spectrum maxima (λ_{max}) shift method." In general, if a 3-, 5- or 4′-OH of a flavonol is glucuronidated, the hypsochromic shifts (i.e. to shorter wavelength) were observed in either Band I (300–380 nm) or Band II (240–280 nm). The resulting shift in Band I associated with the substitution of 3-OH group was in the order of 13~30 nm. Substitution of 5-OH group resulted in a 5~15 nm shift in Band II, and glucuronidation of 4′-OH group produced a 5~10 nm shift in Band I. In contrast, substitution of the hydroxyl group at position C7 had minimal or no effect on the λ_{max} of the UV spectrum (Fig. 2). The above three methods are considered essential and complementary in structural elucidation of glucuronide generated from flavonoids with multiple conjugation sites. The hydrolysis by β-D-glucuronidase is used to confirm β-glucuronide without knowing the number of glucuronic acids attached, whereas MS/MS can detect the number of

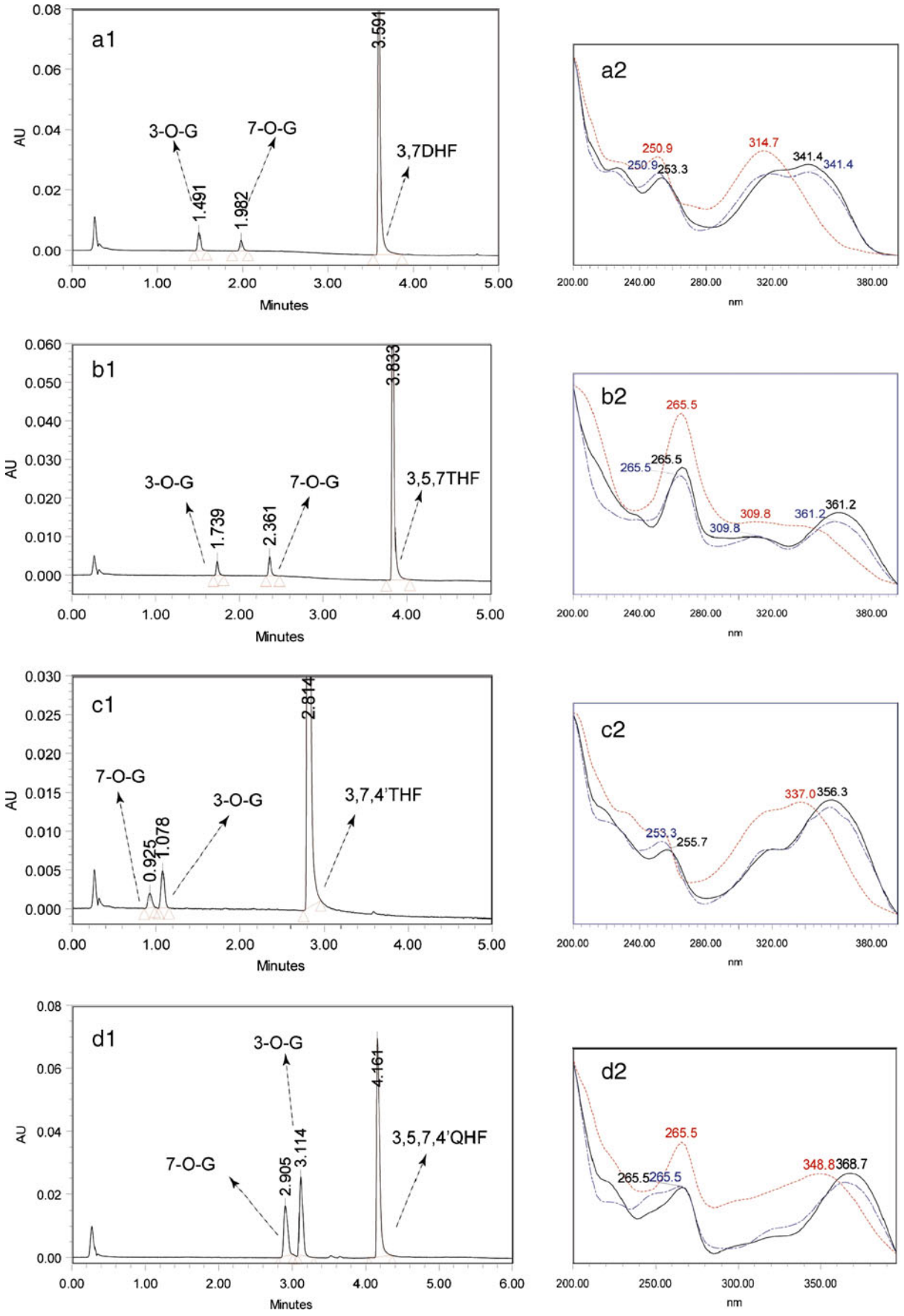
a1
3-O-G
7-O-G
3,7DHF
1.491
1.982
3.591
AU
Minutes
a2
250.9
253.3
314.7
341.4
nm
b1
3-O-G
7-O-G
3,5,7THF
1.739
2.361
3.833
b2
265.5
309.8
361.2
c1
7-O-G
3-O-G
3,7,4'THF
0.925
1.078
2.814
c2
253.3
255.7
337.0
356.3
d1
3-O-G
7-O-G
3,5,7,4'QHF
2.905
3.114
4.161
d2
265.5
348.8
368.7

◀ **Fig. 2** Representative UPLC chromatograms (left) and UV spectra (right) of flavonols and their 3-*O*- / 7-*O*-glucuronides. (**a**–**d**) panels represent 3,7DHF, 3,5,7THF, 3,7,4′THF and 3,5,7,4′-QHF and their 3-*O*- / 7-*O*-glucuronides, respectively. UPLC samples were from enzyme assays in which each flavonol (10 μM) was incubated with 27.5 μg/ml UGT1A9 for 10 or 60 mins. For spectra, black solid line denotes the flavonols, red dotted lines are 3-*O*-glucuronides, and blue dash-dotted lines are 7-*O*-glucuronides. Compared to the parent compounds, band I of 3-*O*-glucuronides either disappeared or had large hypsochromic shifts (to shorter wavelengths) (e.g. 19.3 ~ 26.7 nm). In contrast, 7-*O*-glucuronides had minimal or no changes in the UV spectrum (26).

substituted glucuronic acids, but it is unable to probe the exact conjugative position. In addition, the structure of 3,7-DHF-7-O-glucuronide was confirmed by NMR spectra (Table S1, Supplementary Material). NMR analysis was not performed for glucuronides generated from other flavonols due to serious difficulty in purifying the glucuronide isomers.

Data Analysis

Kinetic parameters (V_{max}, K_m and K_{si} (substrate inhibition constant)) were estimated by fitting the Michaelis-Menten and/or substrate inhibition equations to the substrate concentrations and initial rates. Similar to glucuronidation rates, V_{max} values were also determined as nmol glucuronide formed/mg Supersomes^{TM} protein/min (or nmol/mg protein/min). Eadie-Hofstee plots (Fig. S1, Supplementary Material) were used as diagnostics for model selection. Data analysis was performed by GraphPad Prism V5 for Windows (GraphPad Software, San Diego, CA). The goodness of fit was evaluated on the basis of R^2 values, RSS (residual sum of squares), RMS (root mean square) and residual plots (27).

For better comparison between UGT isoforms, the catalytic efficiencies (or CL_{int} values) of various UGT isoform-mediated glucuronidation were normalized to UGT1A1 using the relative UGT protein expression level. Then, the relative catalytic efficiencies were determined by arbitrarily assigning the calibrated CL_{int} as 1 for the 3-O-glucuronidation of 3,7DHF by UGT1A1.

Statistical Analysis

Significance of mean comparison was examined base on student's t-test using GraphPad Prism V5 for Windows (GraphPad Software, San Diego, CA). Statistical significance was demonstrated with $p<0.05$.

RESULTS

Relative Expression Level Between the UGT1A Enzymes

Relative expression levels of the six UGT1A isoforms were estimated by the Western blot analysis using an anti-UGT1A antibody (against all UGT1A proteins). Each of the isoforms expressed had a protein of apparent molecular mass of approximately 55 kDa (Fig. 3). The relative expression ratios of UGT1A1 (set as 1), 1A3, 1A7, 1A8, 1A9, and 1A10 were 1:0.82:0.94:1.15:0.87:0.93. The maximal difference was about 1.4 times.

Regioselective Glucuronidation of Flavonols by UGT1A1

Four model flavonols (3,7DHF, 3,5,7THF, 3,7,4′THF and 3,5,7,4′QHF) present four possible glucuronidation sites (i.e., 3-OH, 5-OH, 7-OH and 4′-OH). Only 3-*O*- and 7-*O*-glucuronides were observed at all studied concentrations for all four compounds (Figs. 4, 5, 6, 7, 8 and 9). This is consistent with the fact that both 4′-OH and 5-OH groups are typically inactive for UGT1A-mediated glucuronidation, when a 3-OH or a 7-OH group is also present in the structure (19). The kinetic parameters for 3,7,4′THF glucuronidation by UGT1A3, 1A7, 1A8 and 1A10 were not determined, because the compound was not metabolized by these UGT isoforms.

UGT1A1 consistently generated much more flavonol-7-*O*-glucuronides than 3-*O*-glucuronides over the tested concentration range for 3,7DHF, 3,5,7THF and 3,5,7,4′

b

UGTs	Western blot (IDV*/20 μg)
1A1	13915
1A3	11448
1A7	13113
1A8	16027
1A9	12150
1A10	12936

* IDV=Integrated Density Value

Fig. 3 (**a**) Western blot analysis of UGT expression levels in recombinant human UGT Supersomes™. (**b**) UGT band intensities for the six UGT isoforms.

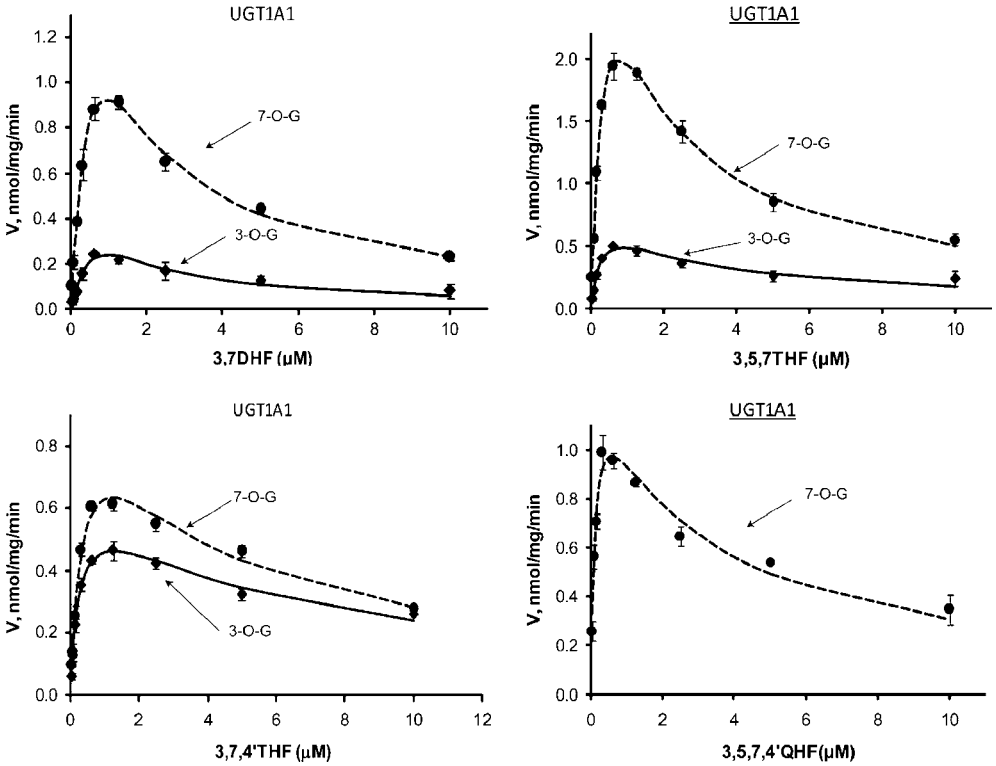

Fig. 4 Kinetics profiles of UGT1A1-mediated glucuronidation of four flavonols (3,7DHF, 3,5,7THF, 3,7,4′THF and 3,5,7,4′QHF). The corresponding Eadie-Hofstee plots are presented in Fig. S1 (Supplementary Materials). For Figs. 3, 4, 5, 6, 7 and 8, solid and dashed lines denote formation rates of flavonol 3-*O*-glucuronides and 7-*O*-glucuronide, respectively. Each data point represents the average of three replicates. Experimental details are presented under Materials and Methods. For kinetic parameters, please see Table II (Figs. 3 and 4) or Table III (Figs. 5, 6, 7 and 8).

Fig. 5 Kinetics profiles of UGT1A3-mediated glucuronidation of three flavonols (3,7DHF, 3,5,7THF and 3,5,7,4′QHF). The corresponding Eadie-Hofstee plots are presented in Fig. S1 (Supplementary Material).

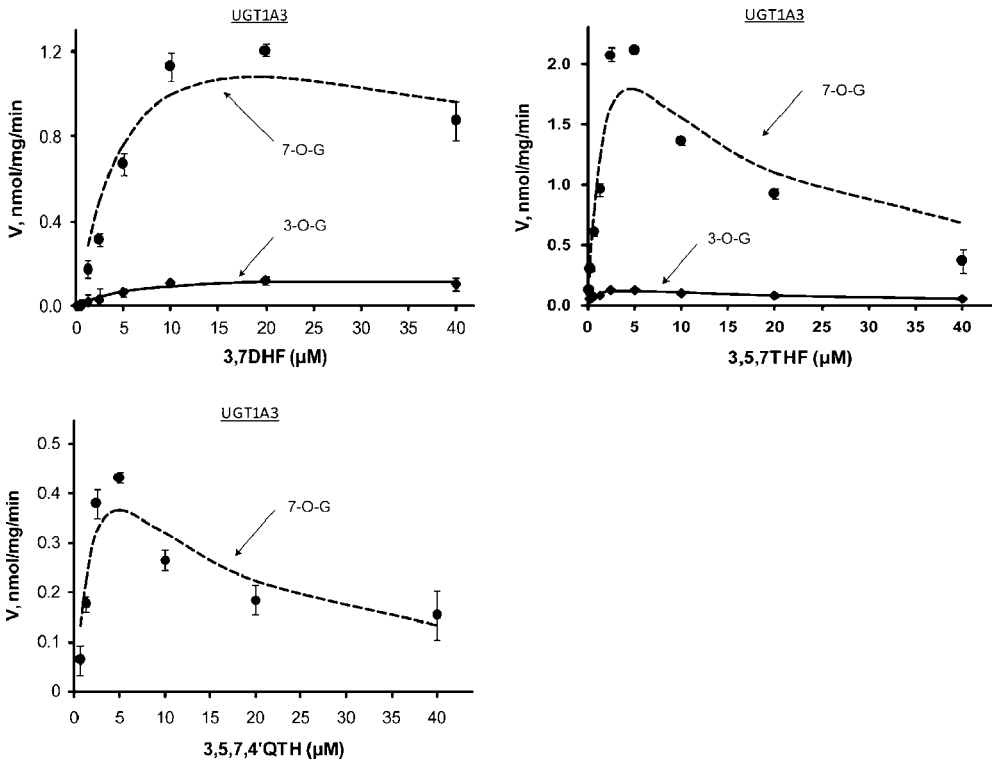

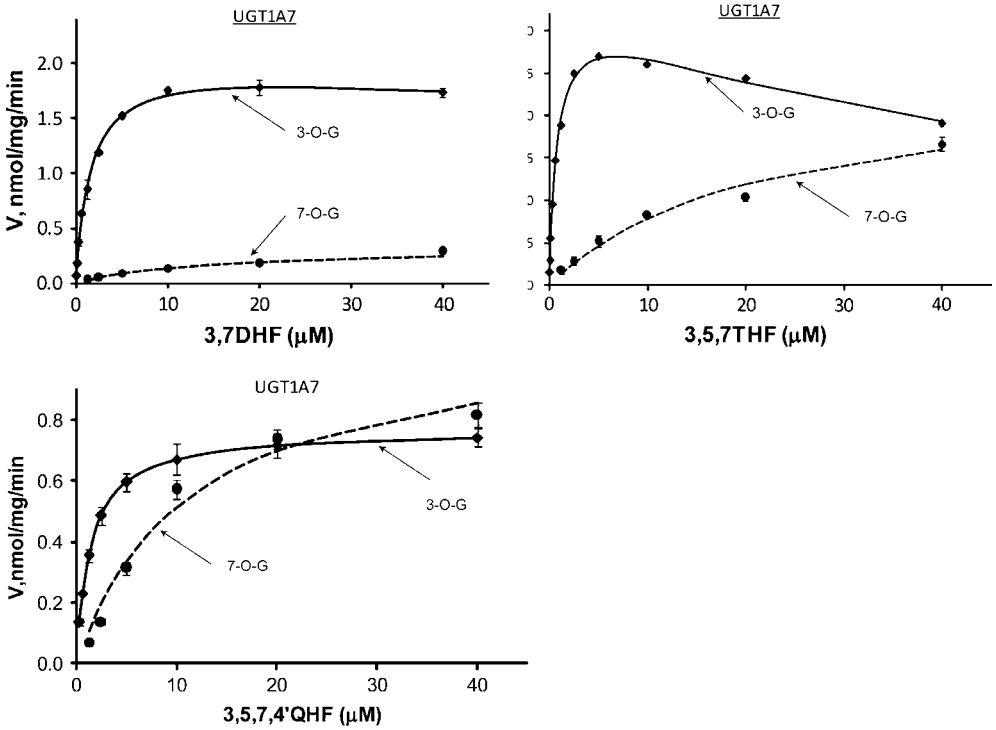

Fig. 6 Kinetics profiles of UGT1A7-mediated glucuronidation of three flavonols (3,7DHF, 3,5,7THF and 3,5,7,4′QHF). The corresponding Eadie-Hofstee plots are presented in Fig. S1 (Supplementary Material).

QHF (Fig. 4). The formation ratios of 7-*O*- /3-*O*-glucuronides fell into the narrow ranges of 3.0-4.2 and 2.3–4.1 for 3,7DHF and 3,5,7THF, respectively (Fig. 10). For 3,5,7,4′ QHF, UGT1A1 only generated 7-O-glucuronide. In the cases of 3,7DHF and 3,5,7THF, the K_m values were similar for 3-*O*- and 7-*O*-glucuronidation, but the differences in V_{max} values were more than 3-fold in favor of 7-*O*-glucuronidation. Therefore, UGT1A1 had much higher

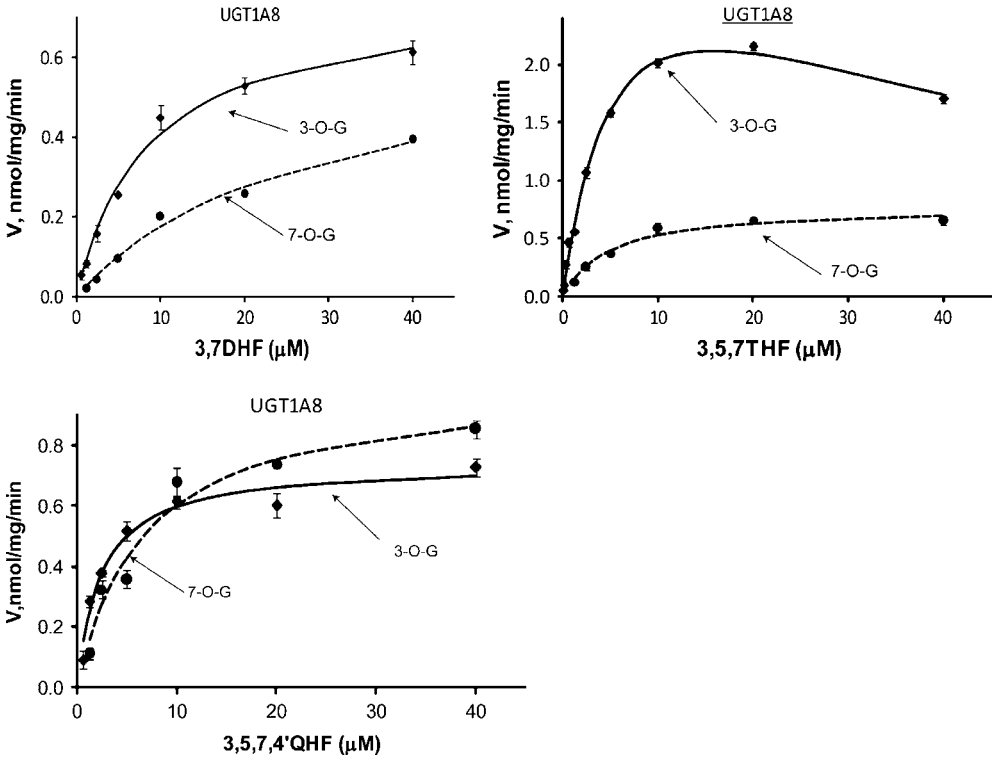

Fig. 7 Kinetics profiles of UGT1A8-mediated glucuronidation of three flavonols (3,7DHF, 3,5,7THF and 3,5,7,4′QHF). The corresponding Eadie-Hofstee plots are presented in Fig. S1 (Supplementary Material).

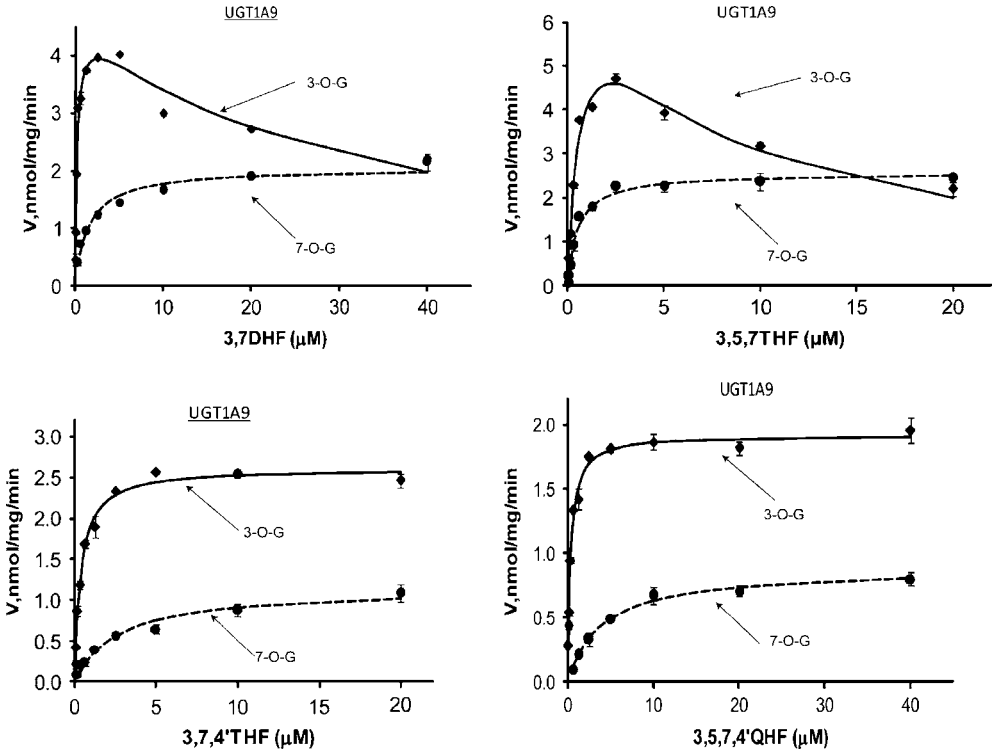

Fig. 8 Kinetics profiles of UGT1A9-mediated glucuronidation of four flavonols (3,7DHF, 3,5,7THF, 3,7,4THF and 3,5,7,4′QHF). The corresponding Eadie-Hofstee plots are presented in Fig. S1 (Supplementary Material).

catalytic efficiency (as reflected by $CL_{int}=V_{max}/K_m$) for 7-OH than that for 3-OH group (greater than 3.4-fold). Together with the fact that the enzyme had the highest binding affinity with 3,5,7,4′QHF but showed a medium V_{max} value, the results suggested that higher binding affinity was not as necessarily associated with higher catalytic capacity (reflected by V_{max} value). For 3,7,4′THF, the formation rates of 7-*O*-glucuronide were slightly higher than those of 3-*O*-

Fig. 9 Kinetics profiles of UGT1A10-mediated glucuronidation of three flavonols (3,7DHF, 3,5,7THF and 3,5,7,4′QHF). The corresponding Eadie-Hofstee plots are presented in Fig. S1 (Supplementary Material).

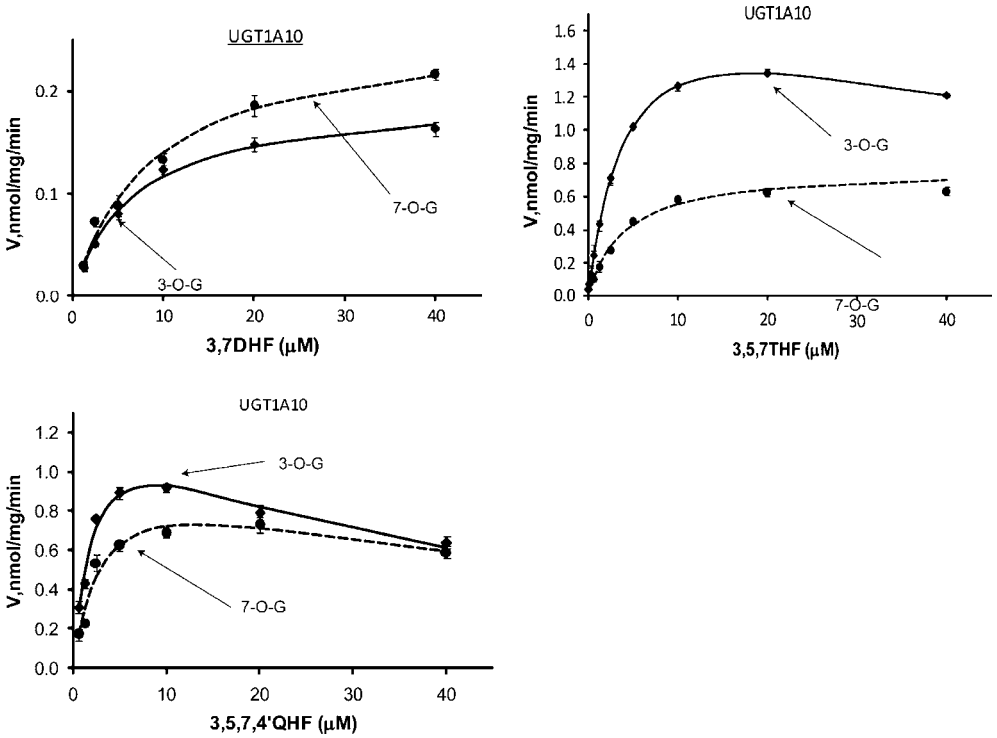

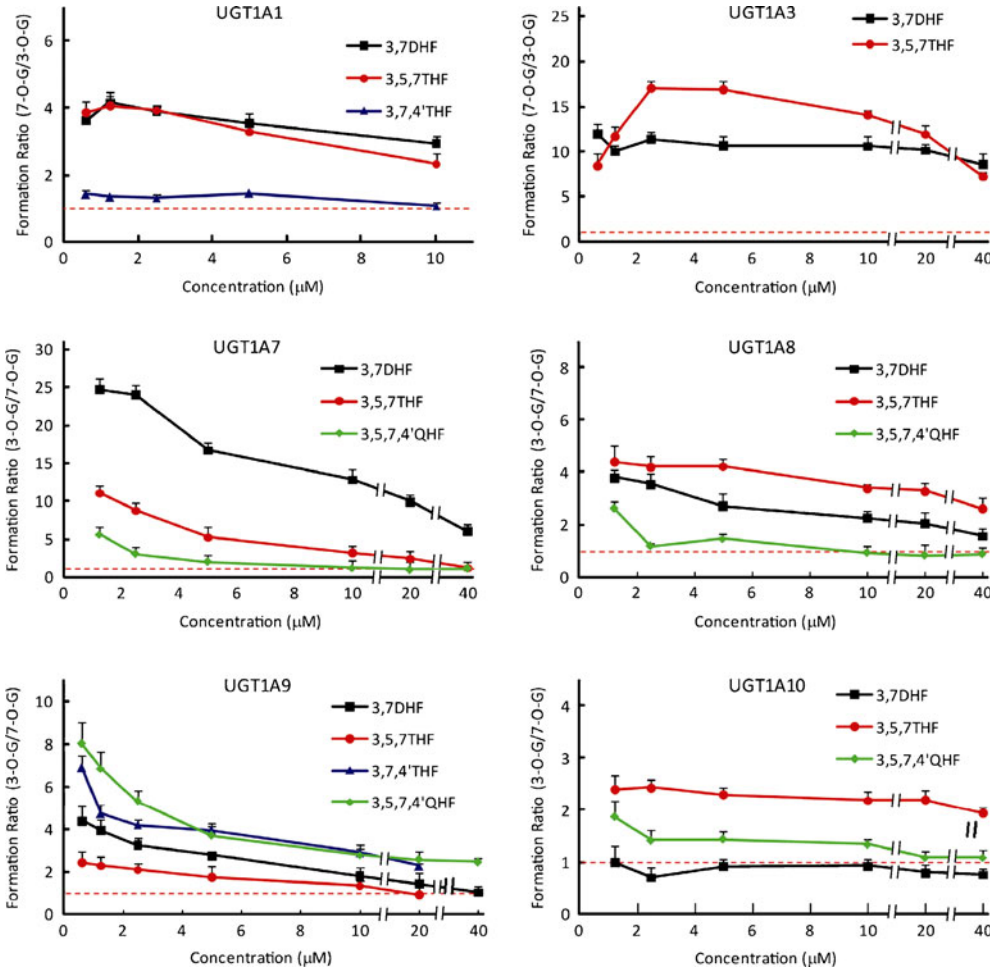

Fig. 10 Formation rate ratios (data transformation from Figs. 4, 5, 6, 7, 8 and 9) between 3-*O*- and 7-*O*-glucuronides catalyzed by UGT1A1, 1A3, 1A7, 1A8, 1A9 and 1A10. For 7-OH preferred enzymes (UGT1A1 and 1A3), the ratios of 7-*O*- over 3-*O*-glucuronidation were plotted against the concentration of corresponding parent compounds, whereas the ratios of 3-O- over 7-O-glucuronidation were plotted for the 3-OH preferred enzymes (UGT1A7-1A10). Reference line of value 1 is shown in red.

glucuronide (Figs. 4 and 10), and the derived kinetic parameters for the positional glucuronidation were similar between these two glucuronides (Table I).

Surprisingly, strong substrate inhibition patterns, as characterized by small K_{si} values (within *in vivo* achievable concentration value) in the range of 0.60–5.4 μM, were observed for both 3-*O*- and 7-*O*-glucuronidation (Table I). The K_m values were in the range of 0.13–1.57 μM, which were much smaller than reported K_m value (49.8 μM) for ethinylestradiol (28). UGT1A1 kinetics towards ethinylestradiol also presented a substrate inhibition profile at high concentrations of UDPGA, which gave the K_{si}/K_m ratio of 1.61. By contrast, the K_{si}/K_m ratios for 3,7DHF were much less than this number, at 0.38 and 1.16 for 3-*O*- and 7-*O*-glucuronidation, respectively.

Regioselective Glucuronidation of Flavonols by UGT1A3

Similar to UGT1A1, UGT1A3 also produced much more flavonol 7-*O*-glucuronides than 3-*O*-glucuronides, and only generated 7-O-glucuronide for 3,5,7,4′QHF (Fig. 5 and Table I). The formation ratios of 7-*O*-/3-*O*-glucuronides were 8.6–11.9 and 7.2–17 for 3,7DHF and 3,5,7THF, respectively (Fig. 10). Likewise, UGT1A3 displayed substrate inhibition kinetics with the regioselective metabolism (Fig. 5 and Table I). The substrate inhibition constants (K_{si}) lay within 7.52–100 μM, significantly larger than those of UGT1A1 ($p<0.05$). The K_m values for UGT1A3-mediated glucuronidation of flavonols varied between 0.84 μM and 8.81 μM. Compared to UGT1A1, UGT1A3 seemed to have even stronger preference for 7-OH metabolism, since the catalytic efficiency ratios (i.e., 7-OH over 3-OH) were up to 13.5 and 8.1 for 3,7DHF and 3,5,7THF, respectively.

Regioselective Glucuronidation of Flavonols by UGT1A7

In contrast to UGT1A1 and 1A3, UGT1A7 more specifically catalyzed formation of flavonol 3-*O*-glucuronide (Fig. 6 and Table II). The differences in rates between 3-*O*- and 7-*O*-glucuronidation decreased markedly with increasing concentration of flavonols (Fig. 10). The formation ratios of 3-*O*- over 7-*O*-glucuronide at 1.25 μM were, respectively, 24.7, 11.0, and 5.6 for 3,7DHF, 3,5,7THF and 3,5,7,4′QHF, whereas those corresponding ratios were 5.9, 1.1 and 1.0 at

Table I The Enzyme Kinetics Parameters for UGT1A1 and 1A3 with Appropriate Flavonols

Enzymes	Substrate/Product(s)	V_{max} nmol/mg protein /min	K_m μM	K_{si} μM	V_{max}/K_m (CL_{int}) ml/mg protein/min
UGT1A1	3,7DHF				
	3-*O*-glucuronide	1.02 ± 0.34	1.57 ± 0.49	0.60 ± 0.38	0.65 ± 0.29
	7-*O*-glucuronide	3.04 ± 0.42	1.04 ± 0.19	1.21 ± 0.23	2.92 ± 0.66
	3,5,7THF				
	3-*O*-glucuronide	0.82 ± 0.14	0.31 ± 0.10	2.64 ± 0.89	2.65 ± 0.96
	7-*O*-glucuronide	4.59 ± 0.46	0.51 ± 0.08	1.22 ± 0.19	9.00 ± 1.67
	3,7,4′THF				
	3-*O*-glucuronide	0.68 ± 0.05	0.30 ± 0.05	5.41 ± 0.93	2.27 ± 0.41
	7-*O*-glucuronide	1.08 ± 0.13	0.43 ± 0.10	3.53 ± 0.86	2.52 ± 0.66
	3,5,7,4′QHF				
	7-*O*-glucuronide	1.38 ± 0.14	0.13 ± 0.03	2.81 ± 0.67	10.6 ± 2.67
UGT1A3	3,7DHF				
	3-*O*-glucuronide	0.18 ± 0.02	8.81 ± 2.72	100 ± 34.8	0.02 ± 0.01
	7-*O*-glucuronide	1.89 ± 0.36	7.02 ± 3.76	50.0 ± 20.2	0.27 ± 0.15
	3,5,7THF				
	3-*O*-glucuronide	0.17 ± 0.01	0.84 ± 0.18	17.9 ± 6.33	0.20 ± 0.04
	7-*O*-glucuronide	3.44 ± 0.84	2.12 ± 1.24	9.95 ± 3.16	1.62 ± 1.02
	3,5,7,4′QHF				
	7-*O*-glucuronide	0.86 ± 0.35	3.30 ± 1.10	7.52 ± 9.58	0.26 ± 0.13

Data are means ± S.E. of three determinations.

40 μM. The differences in CL_{int} values between 3-*O*- and 7-*O*-glucuronidation hit 63.5-, 37.2- and 5.3-folds for 3,7DHF, 3,5,7THF and 3,5,7,4′QHF, respectively. The K_m values for 7-*O*-glcuronidation (11.7–23.2 μM) were much higher than that for 3-*O*-glucuronidation (0.82–1.61 μM), which suggested that the UGT1A7 binding pocket might favor more the binding mode of flavonols for producing 3-*O*-glucuronides than that for generating 7-*O*-glucuronides.

Regioselective Glucuronidation of Flavonols by UGT1A8

The comparisons between formation of flavonol 3-*O*- and 7-*O*-glucuronides revealed that UGT1A8 preferred 3-OH over 7-OH (Fig. 7 and Table II). The degree of regioselectivity between 3-OH and 7-OH varied with the concentration of flavonols. The ratios of 3-O- over 7-O-glucuronidation were 1.5–3.8, 2.6–4.4 and 0.81–2.59 for 3,7DHF, 3,5,7THF and 3,5,7,4′QHF, respectively. The differences in CL_{int} values in terms of 3-OH and 7-O-glucuronidation were >4-fold for 3,7DHF and 3,5,7THF, and >2-fold for 3,5,7,4′QHF.

3-*O*-/7-*O*-glucuronidation was enhanced more than 5.7 times in the presence of a 5-OH group (3,7DHF *vs* 3,5,7THF). However, the addition of a 4′-OH group decreased the catalytic efficiency of 3-*O*-glucuronidation from 0.60 to 0.31 ml/mg protein/min (Table II). The catalytic capacities (V_{max}) for 3,7DHF and 3,5,7,4′QHF were as low as 0.74–0.76 nmol/mg protein/min, much less than the V_{max} value of 3,5,7THF glucuronidation (3.89 nmol/mg protein/min for 3-*O*-glucuornidation).

Regioselective Glucuronidation of Flavonols by UGT1A9

UGT1A9 also preferentially glucuronidated the 3-OH groups of flavonols (Fig. 8 and Table II). The 3-OH preference was more obvious at lower concentrations (Fig. 10). The formation ratio of 3-*O*- over 7-*O*-glucuronide was typically greater than two at concentrations of <2 μM. The catalytic efficiencies of UGT1A9 for 3-OH were more than 14.4-fold higher than that for 7-OH (except 3,5,7THF, which showed a smaller difference at 2.3-fold). The K_m values of 7-*O*-glucuronidation were generally significantly ($p<0.05$) larger than those of 3-*O*-glucuornidation (except for 3,5,7THF, which had similar K_m values). Interestingly, the V_{max} values appeared to be negatively correlated with the K_m values, the K_m values that were less than 1 μM coincided with V_{max} values of higher than 1.9 nmol/mg protein/min (except 7-*O*-glucruonidatin of 3,7DHF). Additionally, 3,7,4′THF was a good substrate for UGT1A9, a fair substrate for UGT1A1, but a non-substrate for 1A3, 1A7, 1A8 or 1A10.

Regioselective Glucuronidation of Flavonols by UGT1A10

UGT1A10 was another UGT1A isoform that prefers 3-O-glucuronidation (Fig. 9 and Table II). This was observed in

Table II The Enzyme Kinetic Parameters for Glucuronidation of Flavonols by 4 UGT1As

Enzymes	Substrate /Product(s)	V_{max} nmol/mg protein /min	K_m μM	K_{si} μM	V_{max}/K_m (CL_{int}) ml/mg protein/min
UGT1A7	3,7DHF				
	3-*O*-glucuronide	2.04 ± 0.07	1.61 ± 0.14	309 ± 127	1.27 ± 0.12
	7-*O*-glucuronide	0.44 ± 0.07	23.2 ± 6.96	N/A	0.02 ± 0.01
	3,5,7THF				
	3-*O*-glucuronide	3.35 ± 0.11	0.82 ± 0.08	55.8 ± 7.27	4.09 ± 0.42
	7-*O*-glucuronide	2.46 ± 0.34	21.4 ± 6.09	N/A	0.11 ± 0.03
	3,5,7,4′QHF				
	3-*O*-glucuronide	0.77 ± 0.04	1.46 ± 0.32	N/A	0.53 ± 0.12
	7-*O*-glucuronide	1.10 ± 0.11	11.6 ± 2.91	N/A	0.10 ± 0.03
UGT1A8	3,7DHF				
	3-*O*-glucuronide	0.76 ± 0.04	8.68 ± 1.21	N/A	0.09 ± 0.01
	7-*O*-glucuronide	0.65 ± 0.10	27.3 ± 7.50	N/A	0.02 ± 0.01
	3,5,7THF				
	3-*O*-glucuronide	3.89 ± 0.47	6.44 ± 1.28	37.3 ± 10.1	0.60 ± 0.14
	7-*O*-glucuronide	0.79 ± 0.27	4.88 ± 1.14	N/A	0.16 ± 0.07
	3,5,7,4′QHF				
	3-*O*-glucuronide	0.74 ± 0.04	2.39 ± 0.47	N/A	0.31 ± 0.06
	7-*O*-glucuronide	1.01 ± 0.09	6.77 ± 1.78	N/A	0.15 ± 0.04
UGT1A9	3,7DHF				
	3-*O*-glucuronide	4.60 ± 0.28	0.22 ± 0.04	30.1 ± 7.11	20.9 ± 4.01
	7-*O*-glucuronide	2.04 ± 0.09	1.50 ± 0.26	N/A	1.36 ± 0.24
	3,5,7THF				
	3-*O*-glucuronide	7.41 ± 0.89	0.68 ± 0.16	7.43 ± 2.12	10.9 ± 2.87
	7-*O*-glucuronide	2.56 ± 0.10	0.54 ± 0.08	N/A	4.74 ± 0.73
	3,7,4′THF				
	3-*O*-glucuronide	2.62 ± 0.05	0.36 ± 0.03	N/A	7.28 ± 0.62
	7-*O*-glucuronide	1.15 ± 0.08	2.67 ± 0.56	N/A	0.43 ± 0.10
	3,5,7,4′QHF				
	3-*O*-glucuronide	1.92 ± 0.03	0.32 ± 0.03	N/A	6.00 ± 0.57
	7-*O*-glucuronide	0.87 ± 0.05	3.87 ± 0.59	N/A	0.22 ± 0.04
UGT1A10	3,7DHF				
	3-*O*-glucuronide	0.19 ± 0.01	6.66 ± 0.66	N/A	0.03 ± 0.00
	7-*O*-glucuronide	0.26 ± 0.02	8.74 ± 1.37	N/A	0.03 ± 0.01
	3,5,7THF				
	3-*O*-glucuronide	2.01 ± 0.14	4.49 ± 0.61	73.5 ± 17.8	0.45 ± 0.07
	7-*O*-glucuronide	0.77 ± 0.04	3.96 ± 0.58	N/A	0.19 ± 0.03
	3,5,7,4′QHF				
	3-*O*-glucuronide	1.46 ± 0.16	2.44 ± 0.55	30.0 ± 8.00	0.60 ± 0.15
	7-*O*-glucuronide	1.10 ± 0.20	3.34 ± 1.21	51.4 ± 27.2	0.33 ± 0.14

Data are means ± S.E. of three determinations. N/A means that parameter K_{si} was not available; this was for the cases in which data fitted better to Michaelis-Menten equation.

the regioselective glucuronidation of 3,5,7THF and 3,5,7,4′ QHF (Fig. 10). The ratios of 3-*O*- over 7-*O*-glucuronidation rates were ~2.3 and 1.1–1.9 for 3,5,7THF and 3,5,7,4′ QHF, respectively. The CL_{int} values for 3-*O*-/7-*O*-glucuronidation were 0.45/0.19 ml/mg protein/min for 3,5,7THF, 0.60/0.33 ml/mg protein/min for 3,5,7,4′ QHF. In the absence of 5-OH, the flavonol 3,7DHF was a very poor substrate of UGT1A10 (with V_{max} value less than 0.26 nmol/mg protein/min and CL_{int} value at ~0.03 ml/mg protein/min), whereas 3,7,4′THF was not a

substrate at all. This indicated that 5-OH is critical for the interaction between UGT1A10 and flavonols, although this group itself was not glucuronidated. It is also suggested that these model compounds bind much weaker to UGT1A10 than to UGT1A9, because UGT1A10 exhibited K_m values (ranging from 3.96 to 8.74 μM for 3-*O*-/7-*O*-glucuronidation), that were significantly larger ($p<0.05$) than the K_m values displayed by UGT1A9 (0.22–0.68 μM for 3-*O*-glucuronidation).

Relative Catalytic Efficiencies Between UGT1A Enzymes

Relative catalytic efficiencies of the six UGT1As are summarized in Table III. Based on the protein sequence identity counting the substrate binding domain, UGT1A1 and 1A3, on average, are only approximately 50% identical to each other and to the polypeptides of the UGT1A7-1A10 cluster. By contrast, the polypeptides within UGT1A7-1A10 cluster are 75–92% identical (8) (Supplementary Material Fig. S2). Interestingly, with fewer shared amino acids, UGT1A1 and 1A3 showed great similarity in regioselective glucuronidation of flavonols (7-OH preference), although UGT1A3 was generally less efficient than UGT1A1 in glucuronidating flavonols, as evidenced by lower relative catalytic efficiencies for each flavonol (Table III). On the other hand, the UGT1A7-1A10 cluster which shares much higher sequence identities commonly preferred to metabolize the 3-OH of flavonols. Nevertheless, these isoforms exhibited divergent catalytic efficiency towards the aglycones (Table III). UGT1A9 showed a striking 3-OH preference ratio of >11 in CL_{int}, whereas the rest of enzymes generally glucuronidated flavonols with a moderate 3-OH preference ratio of< 2.1 in CL_{int} with the exception of 3-*O*-glucuronidation of 3,5,7THF by UGT1A7.

DISCUSSION

This paper for the first time elucidated regioselective glucuronidation of four multi-hydroxyl flavonols by six human UGT1A isoforms via kinetics determination utilizing a normalized expressed level. The "hallmarks" (i.e., distinct regioselectivity and/or substrate selectivity) as presented by the glucuronidation patterns (Table III), helped uncover the fact that these UGT1A isoforms do not always have overlapping substrate specificities with respect to regiospecific glucuronidation. The findings are novel in contrast to previous reports that showed extensive overlapping of UGT1A substrate specificity towards flavonoids (12,14,19). For example, 3-hydroxyflavone at 2.5 μM was similarly metabolized by UGT1A1, 1A7, 1A8, 1A9 and 1A10 (19). The current approach holds great promises on identifying those substrates (probes) that are exclusively metabolized by a particular UGT isoform. Because of the prevalence of UGT generic variants, understanding of regiospecificity of UGT isoform-mediated glucuronidation is also very important to anticipate metabolism *in vivo*, and modeling/prediction of glucuronidation in silico. Moreover, results here would greatly assist in enzymatically synthesizing flavonoid glucuronides conjugated at desired position(s) for pharmaceutical and/or analytical purposes, as accumulating *in vitro* and *in vivo* evidences point to the ability of various (regiospecific) flavonoid glucuronides to retain biological activities (29).

The above observations were made using kinetics profiling (specificity and/or regioselectivity) over a wide concentration range. This approach appears to be superior to the more commonly used method of measuring the enzyme activities at a single high substrate concentration (>100 μM) (22,23). Although the latter approach has the advantages of less cost and labor, this practice might generate an erroneous conclusion, if the concentration was not properly chosen. For example, the formation of 3-*O*-glucuronide by UGT1A9 was much faster than that of 7-*O*-glucuronide for 3,7DHF at concentrations of less than 20 μM (Fig. 8). However, no significant regioselectivity between 3-OH and 7-OH was visible, if glucuronidation rates were only determined at a concentration of over 40 μM. The similar observations were made with UGT1A7 metabolism of 3,5,7THF, as well as glucuronidation of 3,5,7,4′QHF by UGT1A7, 1A8 and 1A10. In addition, the

Table III Normalized Catalytic Efficiencies (Based on the Relative UGT1A Expression Levels) of Six Recombinant Human UGT1As in Glucuronidation of Flavonoids. Relative Catalytic Efficiency ($V_{max}/K_m = 1.0$) was Arbitrarily Assigned for the 3-O-glucuronidation of 3,7DHF by UGT1A1

UGT1A	3,7DHF		3,5,7THF		3,7,4′THF		3,5,7,4′QHF	
	3-O-G*	7-O-G*	3-O-G*	7-O-G*	3-O-G*	7-O-G*	3-O-G*	7-O-G*
1A1	1.0	4.5	4.1	13.8	3.5	3.9	0.0	16.3
1A3	0.0	0.5	0.4	3.0	0	0	0.0	0.5
1A7	2.1	0.0	6.7	0.2	0	0	0.9	0.2
1A8	0.1	0.0	0.8	0.2	0	0	0.4	0.3
1A9	36.8	2.4	19.2	8.4	12.8	0.8	10.6	0.4
1A10	0.0	0.0	0.7	0.3	0	0	1.0	0.5

*3-O-G: 3-O-glucuronidation; 7-O-G: 7-O-glucuronidation

kinetics profiling included substrate concentrations less than 1 μM, which is close to the *in vivo* plasma concentration of flavonoids after they are taken orally (4). Therefore, the data might have greater potential to correlate with *in vivo* especially hepatic metabolism.

The kinetics profiling studies indicate that all UGT1A isoforms have more than one binding site for flavonoids, since their glucuronidation of flavonols displayed strong substrate inhibition patterns. To explain this pattern, one model was proposed by Hutzler and Tracy, who advocate a hypothetical two-site binding model, in which one binding site is productive, whereas the other site is inhibitory and operable only at high substrate concentrations (30). Another group of investigators proposed a compulsory ordered bi bi (two substrates and two products) kinetic model to explain substrate inhibition of UGT1As (28). We used a similar approach and showed that UGT1A9 catalyzed glucuronidation of 3,7,4′-trihydroxyflavone indeed followed the identical kinetic model (Supplementary Materials Fig. S3). Therefore, one reasonable explanation of the substrate inhibition was that binding of the aglycone substrate to the enzyme-UDP complex led to a nonproductive dead-end complex that slows the completion of the catalytic cycle (31).

The hypothesis that there are at least two distinct binding modes present in UGT1As is also strongly supported by the fact that positional (3-*O*- or 7-*O*-) glucuronidation always has different kinetic parameters (24). The differentiated K_m (binding affinity) or V_{max} (reflecting turnover (K_{cat})) values in production of the regiospecific glucuronides indicate that the enzymes provide two divergent interacting environments within which a single flavonol may orient differently. This most likely resulted from one very large active site, instead of two separate small active sites, as supported by the use of UGT1A1 homology models (32,33). Taken together, this body of evidences is in strong support of the theorem that there are at least two binding modes for UGT1A-mediated glucuronidation of flavonols, which can be used as the "expert knowledge" for in silico modeling of UGT1A-mediated glucuronidation.

Structure of flavonols could significantly impact the regioselective glucuronidation rates, regardless of how many modes of bindings are present in UGT1As. In general, the preference order was 3-OH or 7-OH>4′-OH>5-OH among the model flavonols, where the 5-OH and 4′-OH groups were relatively inactive for glucuronidation. These two positions remain poorly active even in the absence of more active -OH groups, as reaction rates of eight flavones with only 5 or 4′-OH available for conjugation was much slower than those shown in this paper (Supplementary Materials Table S2). Even though 5-OH or 4′-OH was not glucuronidated itself, the presence of a -OH group at the C4′ or C5 had major but opposite effects on glucuronidation at the 3 or 7-OH position. The addition of 5-OH generally enhanced the UGT1A-mediated conjugation (excluding UGT1A9), as evidenced by the comparisons between 3,7DHF and 3,5,7THF, or between 3,7,4′THF and 3,5,7,4′QHF in catalytic efficiency (Table III). The enhancement was largely ascribed to more efficient formation of the regioselective conjugates (7-*O*-glucuronide for UGT1A1 and 1A3; 3-*O*-glucuronide for UGT1A7, 1A8 and 1A10). The significance of 5-OH in isoform-specific glucuronidation at the 3-OH or 7-OH positions were also observed for compounds such as chrysin, wogonin, oroxylin A, and 3,5-dihydroxyflavone (15,19). On the contrary, the addition of 4′-OH compromised UGT1A3-, 1A7-, 1A8-, and 1A9-mediated glucuronidation by substantially reducing their respective positional glucuronidation (Table III). The fact that 3-*O*- or 7-*O*-glucuronidation was reduced in the presence of 4′-OH was also supported by the observation that 3-*O*-glucuronidation of 3,4′-dihydroxyflavone was slower than 3-hydroxyflavone at three different concentrations (19).

In conclusion, among the six UGT1As (UGT1A1, 1A3, 1A7, 1A8, 1A9 and 1A10), UGT1A1 and UGT1A9 were the most efficient conjugating enzymes with the smallest K_m values (≤1 μM) and highest intrinsic clearance values. Regardless of their distinctive substrate specificities towards the flavonols, UGT1A1 and 1A3 favored 7-O-glucuornidation, whereas UGT1A7, 1A8, 1A9 and 1A10 preferred 3-O-glucuronidation. The highly different kinetic parameters between 3-*O*- and 7-*O*- glucuronidation suggested that the (at least) two distinct binding modes within the catalytic domain were responsible for the formation of these two glucuronide isomers, which should be considered as useful "expert knowledge" for modeling and predicting UGT1A-mediated glucuronidation. Studies are ongoing to explore these binding modes using homology-based approaches and plant UGT crystal structures.

ACKNOWLEDGMENTS

This work was supported by grants from the National Institutes of Health (GM070737) to MH.

REFERENCES

1. Birt DF, Hendrich S, Wang W. Dietary agents in cancer prevention: flavonoids and isoflavonoids. Pharmacol Ther. 2001;90(2–3):157–77.
2. Ross JA, Kasum CM. Dietary flavonoids: bioavailability, metabolic effects, and safety. Annu Rev Nutr. 2002;22:19–34.
3. Chen J, Lin H, Hu M. Metabolism of flavonoids via enteric recycling: role of intestinal disposition. J Pharmacol Exp Ther. 2003;304(3):1228–35.

4. Setchell KD, Brown NM, Desai P, Zimmer-Nechemias L, Wolfe BE, Brashear WT, *et al.* Bioavailability of pure isoflavones in healthy humans and analysis of commercial soy isoflavone supplements. J Nutr. 2001;131(4 Suppl):1362S–75S.
5. Barve A, Chen C, Hebbar V, Desiderio J, Saw CL, Kong AN. Metabolism, oral bioavailability and pharmacokinetics of chemopreventive kaempferol in rats. Biopharm Drug Dispos. 2009;30 (7):356–65.
6. Tukey RH, Strassburg CP. Human UDP-glucuronosyltransferases: metabolism, expression, and disease. Annu Rev Pharmacol Toxicol. 2000;40:581–616.
7. Radominska-Pandya A, Ouzzine M, Fournel-Gigleux S, Magdalou J. Structure of UDP-glucuronosyltransferases in membranes. Methods Enzymol. 2005;400:116–47.
8. Mackenzie PI, Bock KW, Burchell B, Guillemette C, Ikushiro S, Iyanagi T, *et al.* Nomenclature update for the mammalian UDP glycosyltransferase (UGT) gene superfamily. Pharmacogenetics Genomics. 2005;15:677–85.
9. Fisher MB, Paine MF, Strelevitz TJ, Wrighton SA. The role of hepatic and extrahepatic UDP-glucuronosyltransferases in human drug metabolism. Drug Metab Rev. 2001;33(3–4):273–97.
10. Ohno S, Nakajin S. Determination of mRNA expression of human UDP-glucuronosyltransferases and application for localization in various human tissues by real-time reverse transcriptase-polymerase chain reaction. Drug Metab Dispos. 2009;37(1):32–40.
11. Miners JO, Knights KM, Houston JB, Mackenzie PI. *In vitro-in vivo* correlation for drugs and other compounds eliminated by glucuronidation in humans: pitfalls and promises. Biochem Pharmacol. 2006;71(11):1531–9.
12. Miners JO, Mackenzie PI, Knights KM. The prediction of drug-glucuronidation parameters in humans: UDP-glucuronosyltransferase enzyme-selective substrate and inhibitor probes for reaction phenotyping and *in vitro-in vivo* extrapolation of drug clearance and drug-drug interaction potential. Drug Metab Rev. 2010;42 (1):189–201.
13. Aprile S, Del Grosso E, Grosa G. Identification of the human UDP-glucuronosyltransferases involved in the glucuronidation of combretastatin A-4. Drug Metab Dispos. 2010;38(7):1141–6.
14. Tang L, Singh R, Liu Z, Hu M. Structure and concentration changes affect characterization of UGT isoform-specific metabolism of isoflavones. Mol Pharm. 2009;6(5):1466–82.
15. Zhou Q, Zheng Z, Xia B, Tang L, Lv C, Liu W, *et al.* Use of Isoform-Specific UGT Metabolism to Determine and Describe Rates and Profiles of Glucuronidation of Wogonin and Oroxylin A by Human Liver and Intestinal Microsomes. Pharm Res. 2010;27(8):1568–83.
16. Sorich MJ, Smith PA, Miners JO, Mackenzie PI, McKinnon R. Recent advances in the in silico modelling of UDP glucuronosyltransferase substrates. Curr Drug Metab. 2008;9(1):60–9.
17. Sorich MJ, Smith PA, McKinnon RA, Miners JO. Pharmacophore and quantitative structure activity relationship modelling of UDP-glucuronosyltransferase 1A1 (UGT1A1) substrates. Pharmacogenetics. 2002;12(8):635–45.
18. Smith PA, Sorich MJ, McKinnon RA, Miners JO. In silico insights: chemical and structural characteristics associated with uridine diphosphate glucuronosyltransferase substrate selectivity. Clin Exp Pharmacol Physiol. 2003;30(11):836–40.
19. Tang L, Ye L, Singh R, Wu B, Zhao J, Lv C, *et al.* Use of Glucuronidation Fingerprinting to Describe and Predict mono- and di- Hydroxyflavone Metabolism by Recombinant UGT Isoforms and Human Intestinal and Liver Microsomes. Mol Pharm. 2010;7(3):664–79.
20. Chohan KK, Paine SW, Waters NJ. Quantitative structure activity relationships in drug metabolism. Curr Top Med Chem. 2006;6(15):1569–78.
21. Wong YC, Zhang L, Lin G, Zuo Z. Structure-activity relationships of the glucuronidation of flavonoids by human glucuronosyltransferases. Expert Opin Drug Metab Toxicol. 2009;5 (11):1399–419.
22. Boersma MG, van der Woude H, Bogaards J, Boeren S, Vervoort J, Cnubben NH, *et al.* Regioselectivity of phase II metabolism of luteolin and quercetin by UDP-glucuronosyl transferases. Chem Res Toxicol. 2002;15(5):662–70.
23. Davis BD, Brodbelt JS. Regioselectivity of human UDP-glucuronosyl-transferase 1A1 in the synthesis of flavonoid glucuronides determined by metal complexation and tandem mass spectrometry. J Am Soc Mass Spectrom. 2008;19(2):246–56.
24. Miners JO, Smith PA, Sorich MJ, McKinnon RA, Mackenzie PI. Predicting human drug glucuronidation parameters: application of *in vitro* and in silico modeling approaches. Annu Rev Pharmacol Toxicol. 2004;44:1–25.
25. Wu B, Morrow J, Singh R, Zhang S, Hu M. Three-Dimensional Quantitative Structure-Activity Relationship Studies on UGT1A9-Mediated 3-O-Glucuronidation of Natural Flavonols Using a Pharmacophore-Based Comparative Molecular Field Analysis Model. J Pharmacol Exp Ther. 2011;336(2):403–13.
26. Singh R, Wu BJ, Tang L, Liu ZQ, Hu M. Identification of the Position of Mono-O-Glucuronide of Flavones and Flavonols by Analyzing Shift in Online UV Spectrum (λmax) Generated from an Online Diode-arrayed Detector. J Agric Food Chem. 2010;58 (17):9384–95.
27. Christopoulos A, Lew MJ. Beyond eyeballing: fitting models to experimental data. Crit Rev Biochem Mol Biol. 2000;35(5):359–91.
28. Luukkanen L, Taskinen J, Kurkela M, Kostiainen R, Hirvonen J, Finel M. Kinetic characterization of the 1A subfamily of recombinant human UDP-glucuronosyltransferases. Drug Metab Dispos. 2005;33(7):1017–26.
29. Williamson G, Barron D, Shimoi K, Terao J. *In vitro* biological properties of flavonoid conjugates found *in vivo*. Free Radic Res. 2005;39(5):457–69.
30. Hutzler JM, Tracy TS. Atypical kinetic profiles in drug metabolism reactions. Drug Metab Dispos. 2002;30(4):355–62.
31. Segel IH. Enzyme kinetics: behavior and analysis of rapid equilibrium and steady state enzyme systems, New edn. New York: Wiley; 1993.
32. Li C, Wu Q. Adaptive evolution of multiple-variable exons and structural diversity of drugmetabolizing enzymes. BMC Evol Biol. 2007;7:69.
33. Laakkonen L, Finel M. A molecular model of the human UGT1A1, its membrane orientation and the interactions between different parts of the enzyme. Mol Pharmacol. 2010;77(6):931–9.